Geophysical Research Letters

RESEARCH LETTER
10.1029/2023GL105435

Key Points:

- An ocean/sea-ice/ice-shelf model reveals intensified basal meltwater provokes dynamic changes in ocean currents and sea ice distribution
- The change in transport results in sea ice anomalies consistent with observations near the West Antarctic and Ross Sea coast before 2016
- Basal meltwater is generally not included in climate models which might explain why the models fail to reproduce the observed sea ice trend

Supporting Information:

Supporting Information may be found in the online version of this article.

Correspondence to:

W. G. C. Huneke,
wilma.huneke@anu.edu.au

Citation:

Huneke, W. G. C., Hobbs, W. R., Klocker, A., & Naughten, K. A. (2023). Dynamic response to ice shelf basal meltwater relevant to explain observed sea ice trends near the Antarctic continental Shelf. *Geophysical Research Letters*, *50*, e2023GL105435. https://doi.org/10.1029/2023GL105435

Received 14 AUG 2023
Accepted 24 NOV 2023

Author Contributions:

Conceptualization: Wilma G. C. Huneke, Andreas Klocker
Formal analysis: Wilma G. C. Huneke, William R. Hobbs
Methodology: Wilma G. C. Huneke, Andreas Klocker, Kaitlin A. Naughten
Visualization: Wilma G. C. Huneke
Writing – original draft: Wilma G. C. Huneke, William R. Hobbs
Writing – review & editing: Wilma G. C. Huneke, William R. Hobbs, Andreas Klocker, Kaitlin A. Naughten

Dynamic Response to Ice Shelf Basal Meltwater Relevant to Explain Observed Sea Ice Trends Near the Antarctic Continental Shelf

Wilma G. C. Huneke[1], William R. Hobbs[2], Andreas Klocker[3], and Kaitlin A. Naughten[4]

[1]Research School of Earth Sciences and ARC Centre of Excellence for Climate Extremes, Australian National University, Canberra, ACT, Australia, [2]Australian Antarctic Program Partnership, Institute for Marine and Antarctic Studies, University of Tasmania, Hobart, TAS, Australia, [3]NORCE Norwegian Research Centre, Bjerknes Centre for Climate Research, Bergen, Norway, [4]British Antarctic Survey, Cambridge, UK

Abstract Observed Antarctic sea ice trends up to 2015 have a distinct regional and seasonal pattern, with a loss during austral summer and autumn in the Bellingshausen and Amundsen Seas, and a year-round increase in the Ross Sea. Global climate models generally failed to reproduce the magnitude of sea ice trends implying that the models miss relevant mechanisms. One possible mechanism is basal meltwater, which is generally not included in the current generation of climate models. Previous work on the effects of meltwater on sea ice has focused on thermodynamic processes. However, local freshening also leads to dynamic changes, affecting ocean currents through geostrophic balance. Using a coupled ocean/sea-ice/ice-shelf model, we demonstrate that basal melting can intensify coastal currents in West Antarctica and the westward transport of sea ice. This change in transport results in sea ice anomalies consistent with observations, and may explain the disparity between climate models and observations.

Plain Language Summary Observed sea ice trends around Antarctica vary throughout the year and from region to region. In particular, there was a sea ice loss in summer in West Antarctica and year-round increase in the Ross Sea up to 2015. Global climate models are not able to reproduce these sea ice trends which is a hint that climate models are missing some important mechanisms in the region. One mechanism that is not included in most climate models is meltwater from the base of floating ice shelves and which spreads into the ocean. Basal meltwater can create a situation where there is less dense water near the ice shelves next to denser waters offshore. Such a lateral density gradient will result in faster ocean flows that redistribute existing sea ice. In this study, we use an ocean model that includes ice shelves as well as sea ice and show that this mechanism can create sea ice anomalies that match the observed trends in West Antarctica and the Ross Sea. Our results suggest that including basal meltwater and its effect on the ocean flow in global climate models is important to reproduce observed sea ice trends.

1. Introduction

Antarctic sea ice cover had a net positive trend from 1979 (when reliable satellite records began) to 2015 (Parkinson, 2019). Although the overall trend was within the range of internal variability (Polvani & Smith, 2013; Zunz et al., 2013), maps of Antarctic sea ice change reveal a distinct regional and seasonal pattern. There was (and continues to be) a negative trend during austral summer and autumn in the Bellingshausen and Amundsen Seas, and a positive trend throughout the seasons in the Ross Sea (Hobbs et al., 2016; J. Liu et al., 2004; Turner et al., 2009), which has since disappeared following drastic declines since 2016 (J. Liu et al., 2023; Parkinson, 2019; Parkinson & DiGirolamo, 2021). Global climate models generally fail to reproduce the spatial variability in sea ice trends, and in particular the strong positive trend in the western Ross Sea (between 180°W and Oates Land) is not simulated in any CMIP5 or CMIP6 historical simulations (Hobbs et al., 2015, 2016; Purich et al., 2016; Shu et al., 2020), implying that the models are missing important mechanisms.

Sea ice is at the interface between the atmosphere and the ocean and is therefore subject to dynamic and thermodynamic interactions with both climate system components. Observed West Antarctic sea ice trends are strongly linked to surface meridional wind changes (P. R. Holland & Kwok, 2012; Hosking et al., 2013; Raphael et al., 2019; Turner et al., 2009), which in turn are largely driven by decadal variability in the tropical Pacific (P. R. Holland et al., 2022; Meehl et al., 2016). However, the western Ross Sea trend is only partially explained

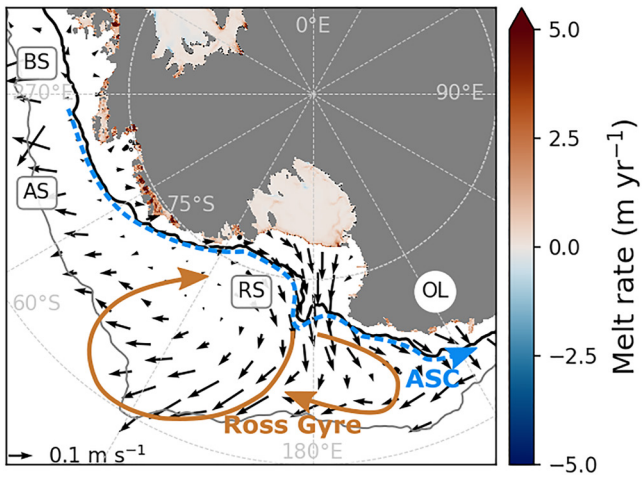

Figure 1. Overview of the study region. Land is in gray, shading shows simulated annual mean basal melt rates and arrows indicate winter sea ice motion in CONTROL. The gray contour indicates a sea ice concentration value of 0.15 and approximates the sea ice edge. The black contour is the 1,000-m isobath and approximates the continental slope. BS stands for Bellingshausen Sea, AS for Amundsen Sea, RS for Ross Sea, and OL for Oates Land. The Antarctic Slope Current is schematically shown in blue and the Ross Gyre in brown.

by wind changes (Hobbs et al., 2016; M. M. Holland et al., 2017), so atmospheric drivers alone do not account for the discrepancy between models and observations.

An important mechanism involving the ocean is the positive ice-ocean feedback which amplifies any initial sea ice perturbation and consequently enhances regional variations (Goosse & Zunz, 2014). A key feature of the polar ocean is that cold surface water rests on top of warmer deep waters, a situation that is maintained because ocean buoyancy in the polar waters is dominated by salinity rather than temperature (Carmack, 2007; Roquet et al., 2022; K. D. Stewart & Haine, 2016). Brine rejection during sea ice production causes surface waters to sink, which entrains warm deeper waters into the mixed layer; a vertical heat flux that limits Antarctic sea ice growth (Martinson, 1998). Hence, any surface freshening that increases stratification—for example, a surplus of sea ice transport into a region that subsequently melts—reduces the vertical heat flux during sea ice growth, leading to more ice production. Lecomte et al. (2017) present observational evidence of the ice-ocean feedback mechanism in the Ross Sea sector without identifying the cause for an initial perturbation.

We propose that the regional pattern of sea ice trend in West Antarctica is related to increased ice shelf basal melting in the region (Adusumilli et al., 2020; Rignot et al., 2019; Wingham et al., 2006). Previous studies have focused on the thermodynamic influence of basal meltwater, specifically by changing the vertical salinity gradient through surface freshening, with considerably varying results between studies (Beadling et al., 2022; Bintanja et al., 2013, 2015; Bronselaer et al., 2018; Hellmer, 2004; Mackie et al., 2020; Merino et al., 2018; Pauling et al., 2016, 2017; Rye et al., 2020; Swart & Fyfe, 2013). Using a model that resolves ice shelf cavities to perform an idealized meltwater perturbation experiment, we suggest that an increase in basal melt rates can indeed contribute to the observed regional sea ice trends, but primarily via a change in ocean dynamics. Specifically, since basal meltwater input is confined to the coast, it changes not only the vertical density gradients, but also has the capacity to incur strong horizontal gradients and accelerate the geostrophic Antarctic Slope Current (ASC, Figure 1) along the continental shelf break (Beadling et al., 2022; Moorman et al., 2020; Nakayama et al., 2014; Naughten, Meissner, Galton-Fenzi, England, Timmermann, & Hellmer, 2018; Thompson et al., 2020). The acceleration of the ASC in turn impacts the westward transport of sea ice and can set the initial perturbation to put the ice-ocean feedback into motion.

2. Methods

2.1. Observations

Sea ice observations are taken from the National Oceanic and Atmospheric Administration/National Snow and Ice Data Center (NSIDC) Climate Data Record for Passive Microwave Sea Ice Concentration (Meier et al., 2013). We calculate changes in sea ice concentration from 1992 to 2011 as the mean seasonal trend multiplied by the total number of years to compare the observations to anomalies in a model perturbation relative to its control simulation (see next section). The seasons are defined as summer (December–February), autumn (March–May), winter (June–August), and spring (September–November).

2.2. MetROMS-Iceshelf

We use the coupled ocean/sea-ice/ice-shelf model MetROMS-iceshelf with a 0.25° horizontal resolution on a circumpolar Antarctic domain as described in Naughten et al. (2017) and Naughten, Meissner, Galton-Fenzi, and England (2018). Basal melting is calculated beneath the ice shelves using a three-equation formulation for the conservation of heat and salinity (Hellmer & Olbers, 1989; D. M. Holland & Jenkins, 1999) with velocity-dependent exchange coefficients for heat and salt. The reference simulation (CONTROL) is the same as in Naughten, Meissner, Galton-Fenzi, and England (2018), which is initialized with ocean temperature and

salinity fields from the ECCO2 state estimate (Menemenlis et al., 2008; Wunsch et al., 2009) and the sea ice field from NSIDC for January 1992. We use 20 years of model integration (1992–2011, 10 years of spin-up and 10 years of analysis period) driven by the ERA-Interim atmospheric reanalysis product (Dee et al., 2011) and an additional surface freshwater flux that accounts for iceberg melt (Martin & Adcroft, 2010). The surface salinity is restored to World Ocean Atlas 2013 monthly climatology (Zweng et al., 2013) with the exception of the Antarctic continental shelf (south of 60°S and shallower than 1,500 m), allowing a free response to simulated basal melting near the coast.

Additional to CONTROL, we conduct an idealized perturbation experiment (FRESH) designed to test the effect of an artificially increased basal freshwater flux on the ocean/sea-ice system. The perturbation involves a simple modification in the model code: the salt flux that the model calculates at the base of the ice shelves due to melting or freezing is subsequently multiplied by a factor of two. Because basal melting is more abundant than freezing, our approach on balance results in a larger freshwater flux into the ocean. The atmospheric forcing and the prescribed surface freshwater flux from iceberg melting remain the same as in the reference simulation. FRESH branches from CONTROL in 2002 after 10 years of model integration which is long enough to equilibrate basal melt rates, and ocean-sea ice state on the Antarctic continental shelf which is the region of interest in this study (Naughten, Meissner, Galton-Fenzi, & England, 2018). The sea ice anomalies of interest emerge in the first 2 years in FRESH and stabilize over the remainder of the simulation (Figure S1 in Supporting Information S1). We analyze the seasonal climatology over the final 3 years (December 2008 to November 2011) of each simulation.

To put the strength of the applied perturbation into context, we compare the basal melt rates in CONTROL and FRESH. The total (circumpolar) melt rate in CONTROL is 629 Gt yr^{-1}, considerably lower than satellite-derived estimates which vary between 1,090 $\pm$ 150 Gt yr^{-1} in 1994 and 1,570 $\pm$ 140 Gt yr^{-1} in 2009 (Adusumilli et al., 2020; Depoorter et al., 2013; Y. Liu et al., 2015; Rignot et al., 2013). CONTROL underestimates particularly the melt rates for small ice shelves which are not well resolved by the model and many of which are in West Antarctica (Naughten, Meissner, Galton-Fenzi, & England, 2018). The total melt rate increases in FRESH to 1,850 Gt yr^{-1} which equals to an addition of 1,221 Gt yr^{-1} (0.04 Sv, where 1 Sv = 3.154×10^4 Gt yr^{-1}). The increase in melt rate is comparable to conservative projections (RCP4.5 scenario) of 1,325 Gt yr^{-1} by 2100 (Golledge et al., 2019) but FRESH only exceeds the observed variability in Antarctic melt rates by about 300 Gt yr^{-1}. Note that the reported melt rate in FRESH is double the simulated melt rate. We report the doubled melt rate as the salt flux in FRESH is perturbed after the model calculates the melt rate, that is, a doubled melt rate reflects the freshwater forcing of the final salt flux.

The reported melt rate of FRESH is more than doubled compared to CONTROL, because the additional freshwater in FRESH modifies the hydrographic conditions in the ice shelf cavity, altering the cavity circulation, and resulting in feedbacks on the simulated melt rates (Jourdain et al., 2017). The spatial distribution of the perturbation varies around the continent. The amplitude is larger for high melting ice shelves in CONTROL and also depends on the strength of the feedbacks on melt rate in each cavity. The pattern of sea ice change described in the result section is the same for a test simulation where the salt flux is quadrupled instead of doubled, but with a larger amplitude (Figure S2 in Supporting Information S1). We therefore hypothesize that our results hold for slightly weaker perturbations (i.e., within the observed range) with the caveat of weaker amplitudes.

3. Results

3.1. Simulated Sea Ice Changes

We start by comparing the observed (Figures 2a–2d) and simulated (Figures 2e–2h) historic sea ice concentration changes. The model CONTROL correctly simulates a decrease (red) in the western Bellingshausen and Amundsen Seas, but fails to simulate the summer and autumn increase (blue) in sea ice concentration in the western Ross Sea and Ross Gyre (Figures 2e and 2f). We hypothesize that too little simulated freshwater input from basal melting in West Antarctica (Bellingshausen and Amundsen Seas) (Naughten, Meissner, Galton-Fenzi, & England, 2018) could explain the discrepancy in the downstream located Ross Sea. To test this, we make use of the freshwater perturbation experiment FRESH. The melt rates for West Antarctica increase from 198 Gt yr^{-1} in CONTROL to 688 Gt yr^{-1} in FRESH which is just outside of the observed range of 576 $\pm$ 92 Gt yr^{-1} (Rignot et al., 2013).

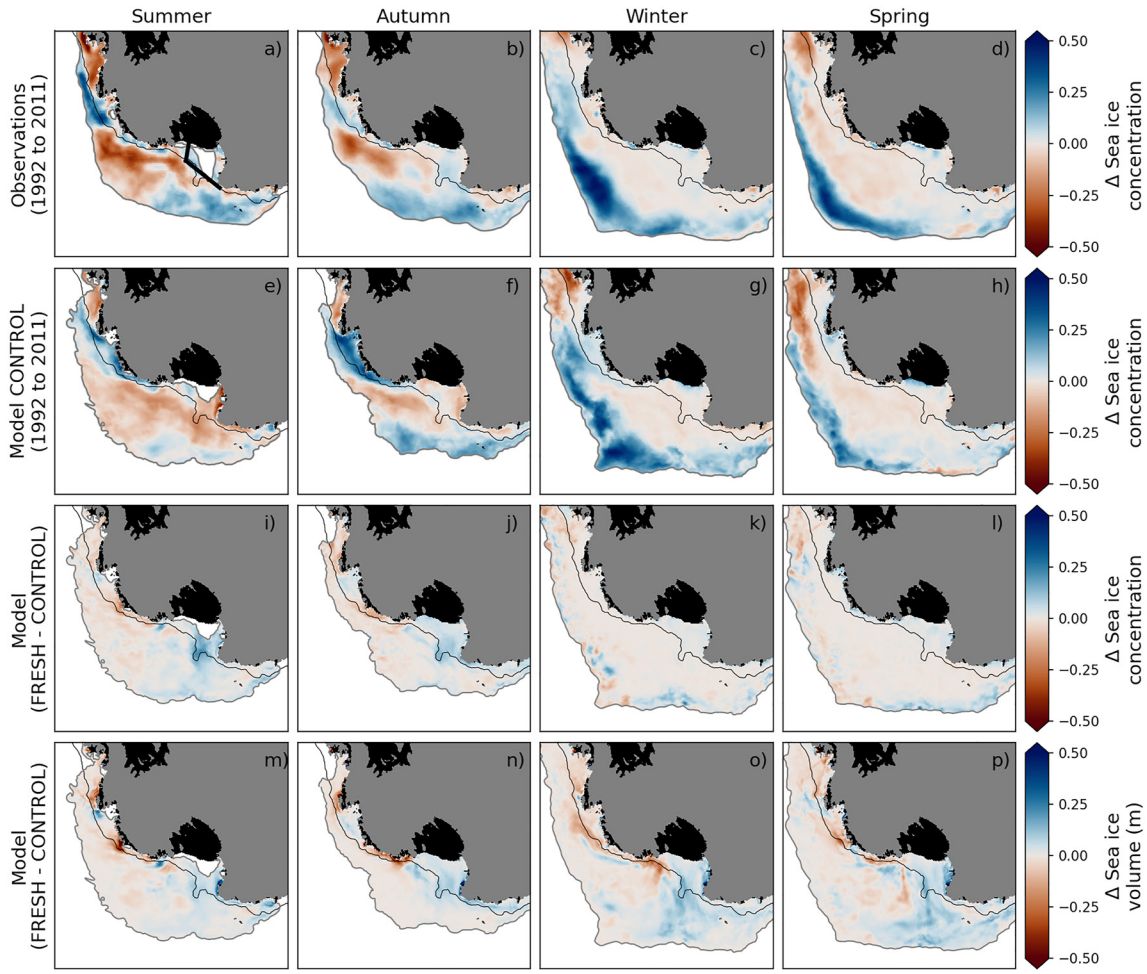

Figure 2. Observed and simulated changes in sea ice. Seasonal change in (a–d) observed and (e–h) simulated sea ice concentration for the time period 1992–2011 calculated as the mean trend multiplied by the total number of years. Seasonal changes in modeled (i–l) sea ice concentration and (m–p) effective sea ice volume (sea ice concentration times sea ice thickness, in units of m) calculated as the difference between FRESH and CONTROL. Red shading indicates a loss in sea ice concentration or volume and blue shading an increase. The black bars indicate the region of the western Ross Sea continental shelf for which area-averaged values are given in Table S1 in Supporting Information S1. The gray contour indicates a sea ice concentration value of 0.15 for CONTROL and approximates the sea ice edge. Values below the 0.15 threshold are masked out. The black contour is the 1,000-m isobath, ice shelves are shaded in black and land in gray.

When compared to CONTROL, the circumpolar integrated sea ice in FRESH increases by 0.7% in area (which is considerably smaller than the 2% ± 0.4% increase in observed sea ice extent from 1979 to 2014 (Parkinson, 2019) as the atmospheric forcing is the same for CONTROL and FRESH and does not generate changes in sea ice) and 3% in volume with large regional variations (Figure S1c and S1f in Supporting Information S1 for anomaly patterns on a circumpolar domain). The spatial pattern of sea ice response to meltwater forcing, calculated as the difference between FRESH and CONTROL, qualitatively matches the observed changes in the western Ross Sea continental shelf and the Ross Gyre (Figures 2a–2d and 2i–2l). The Ross Sea continental shelf signal (area bounded by black bars in Figure 2a), which is largely missing or of opposite sign in the historic CONTROL simulation, is most pronounced in summer and autumn, and is weak or non-existent in winter and spring (Table S1 in Supporting Information S1, first two rows). The seasonality is to be expected as changes in sea ice concentration manifest much more easily in summer when the sea ice pack is less compact; in winter, the ocean surface is fully covered by sea ice so that variance is expressed more in sea ice thickness than area. Changes in sea ice concentration during winter and spring therefore mostly occur near the sea ice edge where the predominantly offshore wind is the dominant transport mechanism (Kimura, 2004), resulting in the overall increase in sea ice area. The decrease in sea ice concentration in the western Bellingshausen and Amundsen Seas is weaker in FRESH compared with the historic CONTROL simulation which suggests the observed decrease in this sector is mostly due to atmospheric forcing.

The simulated response to increased meltwater in summer and autumn (Figures 2i and 2j) is most intense near the coast, where the freshwater perturbation is strongest. However, in the colder months (Figures 2k and 2l) the signal is clearest, although much more modest, at the ice edge in the western Ross Sea. Sea ice volume observations are limited, but the model allows us to additionally investigate the response in sea ice volume to enhanced basal meltwater forcing (Figures 2m–2p, Table S1 in Supporting Information S1 row four). The pattern in volume change resembles to first order the concentration change with decreasing volume in the Bellingshausen and Amundsen Seas and increasing volume in the Ross Sea. Differences occur mostly in the seasonality with sea ice volume signals emerging during winter and spring when the sea ice is consolidated. The negative signal in the Amundsen Sea (confined to the continental shelf) and the positive signal in the western Ross Sea (confined to the continental shelf during summer and autumn and further offshore during winter and spring) persist throughout the year due to decreasing and increasing sea ice thicknesses, respectively.

3.2. Importance of Dynamic Sea Ice Response

The improvements of the sea ice change in FRESH compared to CONTROL on the Ross Sea continental shelf in particular (Table S1 in Supporting Information S1 third row) suggests that basal meltwater forcing may be one of the drivers in this region. To understand how basal meltwater affects sea ice in the model, we consider the sea ice volume tendency and its thermodynamic and dynamic components, both of which are calculated online by the model. The decomposition is informative as the two components represent different physical mechanisms. The thermodynamic sea ice volume tendency component indicates areas of sea ice freezing (Figures S3a–S3d in Supporting Information S1, positive) and melting (Figures S3a–S3d in Supporting Information S1, negative). The dynamic sea ice volume tendency component indicates the redistribution of existing sea ice by convergence (Figures S3e–S3h in Supporting Information S1, positive) and divergence (Figures S3e–S3h in Supporting Information S1, negative). The sea ice volume differences in the final 3 years of the experiment arise from changes in the tendency terms over the entire perturbation period, so to give a direct comparison with Figure 2, we time-integrate the tendency terms over the full perturbation period.

It is important to note that the dynamic and thermodynamic terms are intimately coupled by the sea ice's insulating properties, that is, the presence of sea ice prevents ocean-to-atmosphere heat loss and limits further freeze. Hence, dynamic removal of ice (negative dynamic tendency) allows rapid refreeze (positive thermodynamic tendency). As evident in Figures 3a–3d, the net gain or loss is the residual of these compensating terms. The volume anomaly (Figures 2m–2p) does not exactly match the net volume tendency (Figures 3a–3d) in the respective season as the volume is partially affected by sea ice accumulation from the previous season which results in a noisy field.

In the western Bellingshausen and Amundsen Seas, the dynamic tendency dominates the meltwater response (compare magnitude in Figures 3a–3d and 3i–3l). The dominance of the dynamic tendency emerges in particular in the summer period when the sea ice coverage is less dense and more movable. Accordingly, changes occur mostly in areas along the continental shelf that are already dynamic in CONTROL (Figure S3e in Supporting Information S1 and Figure 3i).

The Ross Sea response is somewhat more complicated since both the dynamic and thermodynamic tendencies are required to explain the net response. There is a dynamic removal of ice from the Ross Sea embayment during the freeze season (Figuress 3j–3l), which allows increased sea ice production (Figures 3f–3h). Some of this ice is transported northwards by winds (Figures 4b–4d), resulting in a positive dynamic response in the outer pack of the western Ross Sea. The greater ice volume at the end of winter means that there is more ice to melt in summer, explaining the negative thermodynamic tendency in the Ross Sea ice edge (Figure 3e), even though there is a positive anomaly in summer ice cover and volume (Figures 2i and 2m). To summarize, dynamical changes in the sea ice volume tendency dominate thermodynamic changes (western Bellingshausen and Amundsen Seas) or are of approximate equal importance (Ross Sea, Table S1 in Supporting Information S1 rows 5–7).

3.3. Basal Meltwater Affects Ocean-Driven Sea Ice Motion

We further analyze the dynamical response to the applied freshwater forcing in FRESH and consider the sea ice and ocean surface motion itself (Figure 4 and Figures S4a–S4d in Supporting Information S1). Sea ice moves westward near the continental shelf in the Bellingshausen and Amundsen Seas as well as west of the Ross Sea

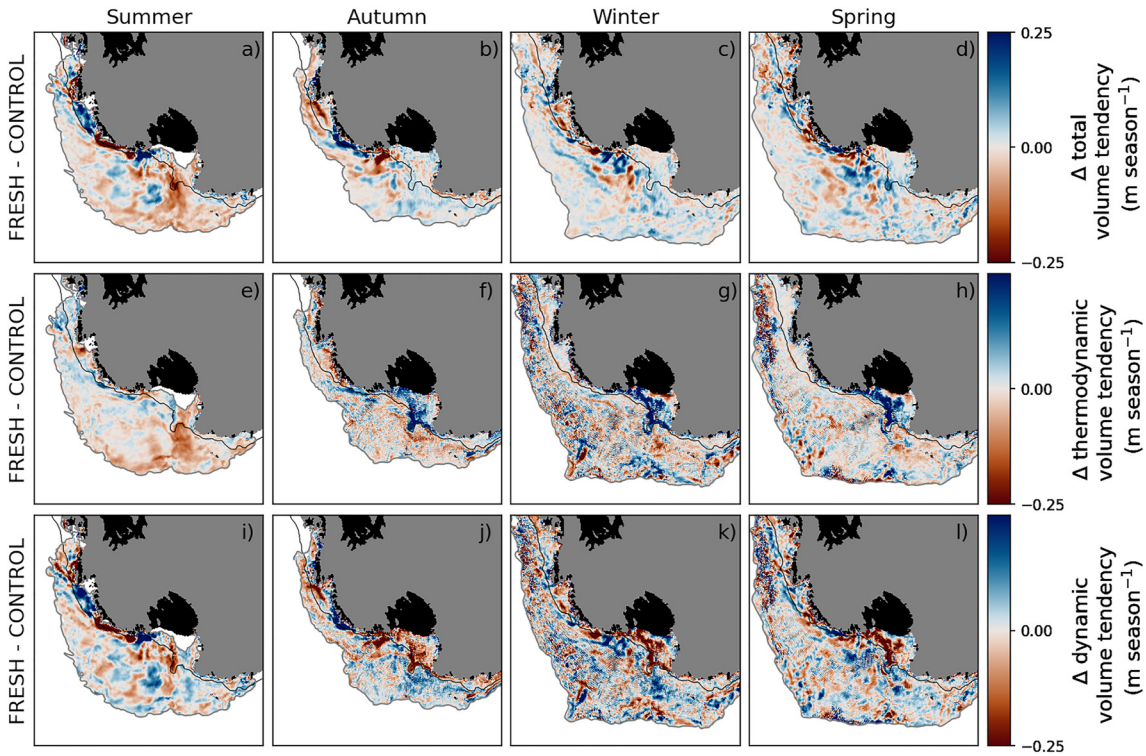

Figure 3. Importance of dynamic sea ice response to increased freshwater input. Seasonal (a–d) total, (e–h) thermodynamic, and (i–l) dynamic sea ice volume tendency changes. In panel (e–h) positive values indicate more sea ice formation and less sea ice melting in FRESH. In panel (i–l) positive values indicate more sea ice convergence and less sea ice divergence in FRESH. The gray contour indicates a sea ice concentration value of 0.15 for CONTROL and approximates the sea ice edge. Values below the 0.15 threshold are masked out. The black contour is the 1,000-m isobath, ice shelves are shaded in black and land in gray.

(Figures 4a–4d). In the Ross Sea, sea ice moves north, that is, away from the coastline, and recirculates to the east in the Ross Gyre. The change in sea ice motion is, however, concentrated in a band along the continental slope (Figures 4e–4h), coinciding with the location of the ASC (Figure 1). Freshwater-driven changes of the ASC therefore explain the regional pattern in sea ice.

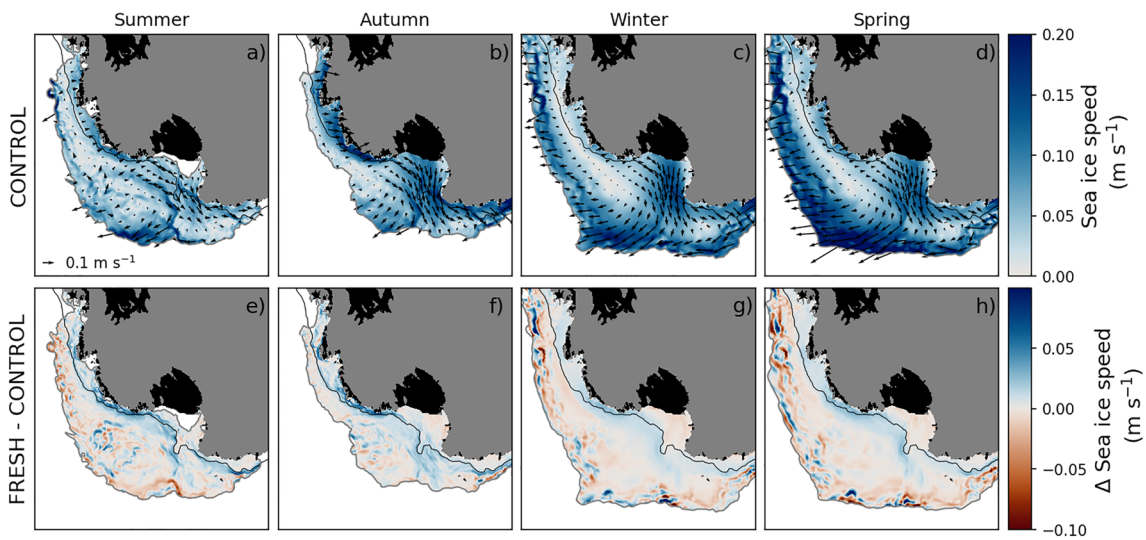

Figure 4. Increased sea ice motion driven by ocean current. (a–d) Seasonal sea ice motion in CONTROL with overlaid arrows that show the strength and direction. (e–h) Difference in sea ice motion between FRESH and CONTROL, positive values indicate larger sea ice velocities in FRESH. The gray contour indicates a sea ice concentration value of 0.15 for CONTROL and approximates the sea ice edge. Values below the 0.15 threshold are masked out. The black contour is the 1,000-m isobath, ice shelves are shaded in black and land in gray.

The additional freshwater in FRESH lowers the continental shelf salinity and with it the density (Figures S5a and S5b in Supporting Information S1). As a consequence, the cross-shelf density gradient strengthens and accelerates the ASC (Figures S4a–S4d in Supporting Information S1). Accordingly, the increase in the velocities is most pronounced downstream of the fast melting ice shelves in the western Bellingshausen and Amundsen Seas (Figure 1). The ASC accelerates most in summer when melt rates peak (Naughten, Meissner, Galton-Fenzi, & England, 2018) and the sea ice concentration is low, which matches the described seasonality in the pattern of sea ice change in the Bellingshausen and Amundsen Seas sector. The stronger current in FRESH favors the redistribution of the sea ice which leads to lower concentrations and allows the surface waters to warm (Figures S4e–S4h in Supporting Information S1).

The acceleration of the ASC is reduced near the Ross Sea embayment, where the geographical conditions differ. The continental shelf is much wider which means the shelf break is further away from the ice shelf where the perturbation is applied. Additionally, the Ross Ice Shelf has low mean melt rates (Figure 1). Both factors result in the applied freshwater perturbation having a smaller effect compared to the neighboring continental shelf which is narrow and adjacent to high melting ice shelves. Downstream of the Ross Sea, where the continental shelf becomes narrow again, the ASC accelerates with similar rates as in the Amundsen Sea.

4. Implications of Sea Ice Redistribution

We propose a new mechanism for the regional variability in observed sea ice trends in West Antarctica. We present evidence from a perturbation experiment in a coupled ocean/sea-ice/ice-shelf model that an increase in ice shelf basal meltwater accelerates the geostrophic ocean circulation which consequently results in the redistribution of the floating sea ice. Our results highlight the crucial role of ocean currents in affecting sea ice distribution, with changes in ocean currents being able to explain some of its observed trends. Sea ice motion is typically associated to the mechanical forcing by winds (P. R. Holland & Kwok, 2012). Our model experiment, however, sets the focus clearly on the ocean circulation as we do not perturb the atmosphere. Our result is consistent with previous studies showing strong westward currents and gyres locally dominate sea ice drift near the coast (Kimura, 2004). Eddy-resolving simulations of the Antarctic margin further show that the momentum transfer between the sea ice and the ocean in the ASC band reduces to almost zero resulting in comparable sea ice and ocean velocities (Si et al., 2021; A. L. Stewart et al., 2018, 2019), which approximately holds in our not fully eddy-resolving simulations (Figures S5c and S5d in Supporting Information S1). Changes in the ocean current due to buoyancy forcing can therefore be expected to be reflected in the sea ice. Our results also agree with existing literature which supports an important role of buoyancy forcing, including that from basal meltwater, for the strength of the ASC (Beadling et al., 2022; Moorman et al., 2020; Nakayama et al., 2014; Naughten, Meissner, Galton-Fenzi, England, Timmermann, & Hellmer, 2018; Thompson et al., 2020).

The redistribution of sea ice that we demonstrate here has broader impacts on the climate and ecosystem. Coastal sea ice has a role in protecting ice shelves from destructive ocean swells (Massom et al., 2018) and summer warming of surface waters in front of the ice shelf (Kusahara, 2021). Our study shows that meltwater from Amundsen Sea ice shelves causes the removal of sea ice away from those same shelves, potentially invoking a positive feedback that could enhance future melt rates. The ecosystem response to Antarctic sea ice change is complex and not well-understood, but there is significant evidence that changes to coastal sea ice (e.g., Amundsen Sea) and the outer pack (e.g., Ross Sea) has implications for primary production, keystone species (e.g., krill) and distributions of iconic megafauna such as penguins (Massom & Stammerjohn, 2010).

An important caveat to the result of this study is that our experiments are run in an uncoupled state that does not allow for atmospheric feedbacks to evolve. In particular, surface air temperature is especially tightly coupled to sea ice concentration (Hobbs et al., 2020; Massonnet et al., 2013), and we expect this to somewhat damp the sea ice concentration response to perturbation and to explain why the amplitude of anomalies in CONTROL alone compare more favorably with observations. However, sea ice thickness is more free to respond to the ocean thermal state and to thickening by dynamic convergence, and indeed we see a stronger response in sea ice volume than concentration.

The response of sea ice to the freshwater from basal melting is sensitive as to how the perturbation is applied in the model, and to the model resolution (Beadling et al., 2022; Bintanja et al., 2013, 2015; Bronselaer et al., 2018; Hellmer, 2004; Mackie et al., 2020; Merino et al., 2018; Pauling et al., 2016, 2017; Rye et al., 2020; Swart &

Fyfe, 2013). Our model configuration benefits from its ability to adequately resolve ocean circulation at the Antarctic margins and that it includes active ice shelves. Most current global climate models lack these two factors, so they likely underestimate the meltwater-driven changes in the ocean circulation and sea ice motion described in this study. Future work should test if the proposed mechanism holds in a coupled model with comparable grid resolution and active ice shelf cavities once such model becomes available. Additionally, a greater consensus between freshwater perturbation experiments with numerical models is desirable to eventually improve future climate simulations.

5. Conclusion

We present a mechanism by which basal meltwater can accelerate west Antarctic coastal currents and redistribute sea ice. This mechanism is distinct from previous similar studies that have focused on how meltwater changes the vertical heat flux that limits sea ice growth. A dynamical response may also be active in earlier models but went undiagnosed. The proposed mechanism removes sea ice from ice shelf fronts of the rapidly melting Amundsen Sea ice shelves. Since previous work suggests that sea ice plays a role in moderating ice shelf mass loss, this mechanism could lead to a positive feedback by removing the protection of coastal sea ice from affected ice shelves, as ice shelf melt accelerates in the near future.

Data Availability Statement

The model source code is available from Naughten (2016). Model output is available from a Zenodo repository at Huneke (2023). Sea ice observations are available from NSIDC (2021). Python scripts for data analysis and for producing figures can be obtained at the Huneke (2022) github repository.

Acknowledgments
This research was supported under the Australian Research Council's Special Research Initiative for Antarctic Gateway Partnership (SR140300001) and the Centre of Excellence for Climate Extremes (CE170100023). Will Hobbs is supported by grant funding from the Australian Government as part of the Antarctic Science Collaboration Initiative program. Andreas Klocker is supported by the Research Council of Norway through project KeyPOCP (Studies of Key Polar Ocean and Climate Processes with high resolution coupled climate models). Kaitlin Naughten's involvement was supported by the Drivers and Effects of Fluctuations in sea Ice in the ANTarctic (DEFIANT) project funded by the Natural Environment Research Council, UK. This research was undertaken on the National Computational Infrastructure (NCI) in Canberra, Australia, which is supported by the Australian Commonwealth Government. Open access publishing facilitated by Australian National University, as part of the Wiley - Australian National University agreement via the Council of Australian University Librarians.

References

Adusumilli, S., Fricker, H. A., Medley, B., Padman, L., & Siegfried, M. R. (2020). Interannual variations in meltwater input to the Southern Ocean from Antarctic ice shelves. *Nature Geoscience*, *13*(9), 616–620. https://doi.org/10.1038/s41561-020-0616-z

Beadling, R. L., Krasting, J. P., Griffies, S. M., Hurlin, W. J., Bronselaer, B., Russell, J. L., et al. (2022). Importance of the Antarctic slope current in the southern ocean response to ice sheet melt and wind stress change. *Journal of Geophysical Research: Oceans*, *127*(5), e2021JC017608. https://doi.org/10.1029/2021JC017608

Bintanja, R., Van Oldenborgh, G. J., Drijfhout, S. S., Wouters, B., & Katsman, C. A. (2013). Important role for ocean warming and increased ice-shelf melt in Antarctic sea-ice expansion. *Nature Geoscience*, *6*(5), 376–379. https://doi.org/10.1038/ngeo1767

Bintanja, R., Van Oldenborgh, G. J., & Katsman, C. A. (2015). The effect of increased fresh water from Antarctic ice shelves on future trends in Antarctic sea ice. *Annals of Glaciology*, *56*(69), 120–126. https://doi.org/10.3189/2015AoG69A001

Bronselaer, B., Winton, M., Griffies, S. M., Hurlin, W. J., Rodgers, K. B., Sergienko, O. V., et al. (2018). Change in future climate due to Antarctic meltwater. *Nature*, *564*(7734), 53–58. https://doi.org/10.1038/s41586-018-0712-z

Carmack, E. C. (2007). The alpha/beta ocean distinction: A perspective on freshwater fluxes, convection, nutrients and productivity in high-latitude seas. *Deep-Sea Research Part II Topical Studies in Oceanography*, *54*(23–26), 2578–2598. https://doi.org/10.1016/j.dsr2.2007.08.018

Dee, D. P., Uppala, S. M., Simmons, A. J., Berrisford, P., Poli, P., Kobayashi, S., et al. (2011). The ERA-Interim reanalysis: Configuration and performance of the data assimilation system. *Quarterly Journal of the Royal Meteorological Society*, *137*(656), 553–597. https://doi.org/10.1002/qj.828

Depoorter, M. A., Bamber, J. L., Griggs, J. A., Lenaerts, J. T. M., Ligtenberg, S. R. M., van den Broeke, M. R., & Moholdt, G. (2013). Calving fluxes and basal melt rates of Antarctic ice shelves. *Nature*, *502*(7469), 89–92. https://doi.org/10.1038/nature12567

Golledge, N. R., Keller, E. D., Gomez, N., Naughten, K. A., Bernales, J., Trusel, L. D., & Edwards, T. L. (2019). Global environmental consequences of twenty-first-century ice-sheet melt. *Nature*, *566*(7742), 65–72. https://doi.org/10.1038/s41586-019-0889-9

Goosse, H., & Zunz, V. (2014). Decadal trends in the Antarctic sea ice extent ultimately controlled by ice-ocean feedback. *The Cryosphere*, *8*(2), 453–470. https://doi.org/10.5194/tc-8-453-2014

Hellmer, H. H. (2004). Impact of Antarctic ice shelf basal melting on sea ice and deep ocean properties. *Geophysical Research Letters*, *31*(10), 1–4. https://doi.org/10.1029/2004GL019506

Hellmer, H. H., & Olbers, D. (1989). A two-dimensional model for the thermohaline circulation under an ice shelf. *Antarctic Science*, *1*(4), 325–336. https://doi.org/10.1017/s0954102089000490

Hobbs, W. R., Bindoff, N. L., & Raphael, M. N. (2015). New perspectives on observed and simulated Antarctic sea ice extent trends using optimal fingerprinting techniques. *Journal of Climate*, *28*(4), 1543–1560. https://doi.org/10.1175/JCLI-D-14-00367.1

Hobbs, W. R., Klekociuk, A. R., & Pan, Y. (2020). Validation of reanalysis Southern Ocean atmosphere trends using sea ice data. *Atmospheric Chemistry and Physics*, *20*(23), 14757–14768. https://doi.org/10.5194/acp-20-14757-2020

Hobbs, W. R., Massom, R., Stammerjohn, S., Reid, P., Williams, G., & Meier, W. (2016). A review of recent changes in Southern Ocean sea ice, their drivers and forcings. *Global and Planetary Change*, *143*, 228–250. https://doi.org/10.1016/j.gloplacha.2016.06.008

Holland, D. M., & Jenkins, A. (1999). Modeling thermodynamic ice–ocean interactions at the base of an ice shelf. *Journal of Physical Oceanography*, *29*(8), 1787–1800. https://doi.org/10.1175/1520-0485(1999)029<1787:mtioia>2.0.co;2

Holland, M. M., Landrum, L., Raphael, M., & Stammerjohn, S. (2017). Springtime winds drive Ross Sea ice variability and change in the following autumn. *Nature Communications*, *8*(1), 731. https://doi.org/10.1038/s41467-017-00820-0

Holland, P. R., & Kwok, R. (2012). Wind-driven trends in Antarctic sea-ice drift. *Nature Geoscience*, *5*(12), 872–875. https://doi.org/10.1038/ngeo1627

Holland, P. R., O'connor, G. K., Bracegirdle, T. J., Dutrieux, P., Naughten, K. A., Steig, E. J., et al. (2022). Anthropogenic and internal drivers of wind changes over the Amundsen Sea, West Antarctica, during the 20th and 21st centuries. *The Cryosphere*, *16*(12), 5085–5105. https://doi.org/10.5194/tc-16-5085-2022

Hosking, J. S., Orr, A., Marshall, G. J., Turner, J., & Phillips, T. (2013). The influence of the Amundsen-Bellingshausen Seas Low on the climate of West Antarctica and its representation in coupled climate model simulations. *Journal of Climate*, *26*(17), 6633–6648. https://doi.org/10.1175/JCLI-D-12-00813.1

Huneke, W. G. C. (2022). Analysis scripts for manuscript "Dynamic response to ice shelf basal meltwater relevant to explain observed sea ice trends near the Antarctic continental shelf" [Python scripts]. Github Repository. Retrieved from https://github.com/wghuneke/MetROMS_BasalMelt_Perturbation

Huneke, W. G. C. (2023). MetROMS model output for manuscript "Dynamic response to ice shelf basal meltwater relevant to explain observed sea ice trends near the Antarctic continental shelf" [Dataset]. Zenodo. https://doi.org/10.5281/zenodo.8245112

Jourdain, N. C., Mathiot, P., Merino, N., Durand, G., Le Sommer, J., Spence, P., et al. (2017). Ocean circulation and sea-ice thinning induced by melting ice shelves in the Amundsen Sea. *Journal of Geophysical Research: Oceans*, *122*(3), 2550–2573. https://doi.org/10.1002/2016JC012509

Kimura, N. (2004). Sea ice motion in response to surface wind and ocean current in the Southern Ocean. *Journal of the Meteorological Society of Japan*, *82*(4), 1223–1231. https://doi.org/10.2151/jmsj.2004.1223

Kusahara, K. (2021). Summertime linkage between Antarctic Sea sea-ice extent and ice-shelf basal melting through Antarctic coastal water masses' variability: A circumpolar southern ocean model study. *Environmental Research Letters*, *16*(7), 074042. https://doi.org/10.1088/1748-9326/ac0de0

Lecomte, O., Goosse, H., Fichefet, T., De Lavergne, C., Barthélemy, A., & Zunz, V. (2017). Vertical ocean heat redistribution sustaining sea-ice concentration trends in the Ross Sea. *Nature Communications*, *8*(1), 258. https://doi.org/10.1038/s41467-017-00347-4

Liu, J., Curry, J. A., & Martinson, D. G. (2004). Interpretation of recent Antarctic sea ice variability. *Geophysical Research Letters*, *31*(2), 2000–2003. https://doi.org/10.1029/2003GL018732

Liu, J., Zhu, Z., & Chen, D. (2023). Lowest Antarctic Sea Ice record broken for the second year in a row. *Ocean-Land-Atmosphere Research*, *2*, 1–2. https://doi.org/10.34133/olar.0007

Liu, Y., Moore, J. C., Cheng, X., Gladstone, R. M., Bassis, J. N., Liu, H., et al. (2015). Ocean-driven thinning enhances iceberg calving and retreat of Antarctic ice shelves. *Proceedings of the National Academy of Sciences of the United States of America*, *112*(11), 3263–3268. https://doi.org/10.1073/pnas.1415137112

Mackie, S., Smith, I. J., Ridley, J. K., Stevens, D. P., & Langhorne, P. J. (2020). Climate response to increasing Antarctic iceberg and ice shelf melt. *Journal of Climate*, *33*(20), 8917–8938. https://doi.org/10.1175/JCLI-D-19-0881.1

Martin, T., & Adcroft, A. (2010). Parameterizing the fresh-water flux from land ice to ocean with interactive icebergs in a coupled climate model. *Ocean Modelling*, *34*(3–4), 111–124. https://doi.org/10.1016/j.ocemod.2010.05.001

Martinson, D. G., & Iannuzzi, R. A. (1998). Antarctic ocean-ice interaction: Implications from ocean bulk property distributions in the Weddell Gyre. *Antarctic Sea Ice: Physical Processes, Interactions and Variability*, *74*, 243–271. https://doi.org/10.1029/ar074p0243

Massom, R. A., Scambos, T. A., Bennetts, L. G., Reid, P., Squire, V. A., & Stammerjohn, S. E. (2018). Antarctic ice shelf disintegration triggered by sea ice loss and ocean swell. *Nature*, *558*(7710), 383–389. https://doi.org/10.1038/s41586-018-0212-1

Massom, R. A., & Stammerjohn, S. E. (2010). Antarctic sea ice change and variability - Physical and ecological implications. *Polar Science*, *4*(2), 149–186. https://doi.org/10.1016/j.polar.2010.05.001

Massonnet, F., Mathiot, P., Fichefet, T., Goosse, H., König Beatty, C., Vancoppenolle, M., & Lavergne, T. (2013). A model reconstruction of the Antarctic sea ice thickness and volume changes over 1980-2008 using data assimilation. *Ocean Modelling*, *64*, 67–75. https://doi.org/10.1016/j.ocemod.2013.01.003

Meehl, G. A., Arblaster, J. M., Bitz, C. M., Chung, C. T., & Teng, H. (2016). Antarctic sea-ice expansion between 2000 and 2014 driven by tropical Pacific decadal climate variability. *Nature Geoscience*, *9*(8), 590–595. https://doi.org/10.1038/ngeo2751

Meier, W. N., Peng, G., Schott, D. J., & Savoie, M. H. (2013). NOAA/NSIDC climate data record of passive microwave sea-ice concentration. *Polar Research*, *33*(1), 21004. https://doi.org/10.3402/polar.v33.21004

Menemenlis, D., Campin, J. M., Heimbach, P., Hill, C., Lee, T., Nguyen, A., et al. (2008). ECCO2: High resolution global ocean and sea ice data synthesis. *Mercator Ocean Quaterly Newsletter*, *31*, 13–21.

Merino, N., Jourdain, N. C., Le Sommer, J., Goosse, H., Mathiot, P., & Durand, G. (2018). Impact of increasing Antarctic glacial freshwater release on regional sea-ice cover in the Southern Ocean. *Ocean Modelling*, *121*, 76–89. https://doi.org/10.1016/j.ocemod.2017.11.009

Moorman, R., Morrison, A. K., & Hogg, A. M. (2020). Thermal responses to Antarctic ice shelf melt in an eddy rich global ocean–sea-ice model. *Journal of Climate*, *33*(15), 6599–6620. https://doi.org/10.1175/jcli-d-19-0846.1

Nakayama, Y., Timmermann, R., Rodehacke, C. B., Schröder, M., & Hellmer, H. H. (2014). Modeling the spreading of glacial meltwater from the Amundsen and Bellingshausen Seas. *Geophysical Research Letters*, *41*(22), 7942–7949. https://doi.org/10.1002/2014GL061600

Naughten, K. A. (2016). MetROMS-iceshelf model source code. *Github Repository*. Retrieved from https://github.com/knaughten/metroms_iceshelf

Naughten, K. A., Galton-Fenzi, B. K., Meissner, K. J., England, M. H., Brassington, G. B., Colberg, F., et al. (2017). Spurious sea ice formation caused by oscillatory ocean tracer advection schemes. *Ocean Modelling*, *116*, 108–117. https://doi.org/10.1016/j.ocemod.2017.06.010

Naughten, K. A., Meissner, K. J., Galton-Fenzi, B. K., England, M. H., Timmermann, R., & Hellmer, H. H. (2018). Future projections of Antarctic ice shelf melting based on CMIP5 scenarios. *Journal of Climate*, *31*(13), 5243–5261. https://doi.org/10.1175/JCLI-D-17-0854.1

Naughten, K. A., Meissner, K. J., Galton-Fenzi, B. K., England, M. H., Timmermann, R., Hellmer, H. H., et al. (2018). Intercomparison of Antarctic ice-shelf, ocean, and sea-ice interactions simulated by MetROMS-iceshelf and FESOM 1.4. *Geoscientific Model Development*, *11*(4), 1257–1292. https://doi.org/10.5194/gmd-11-1257-2018

NSIDC. (2021). Climate data record for passive microwave sea ice concentration from the National Oceanic and Atmospheric Administration/National Snow and ice data Center [Dataset]. NOAA. Retrieved from https://noaadata.apps.nsidc.org/NOAA/G02202_V4/south/monthly/

Parkinson, C. L. (2019). A 40-y record reveals gradual Antarctic sea ice increases followed by decreases at rates far exceeding the rates seen in the Arctic. *Proceedings of the National Academy of Sciences of the United States of America*, *116*(29), 14414–14423. https://doi.org/10.1073/pnas.1906556116

Parkinson, C. L., & DiGirolamo, N. E. (2021). Sea ice extents continue to set new records: Arctic, Antarctic, and global results. *Remote Sensing of Environment*, *267*(September), 112753. https://doi.org/10.1016/j.rse.2021.112753

Pauling, A. G., Bitz, C. M., Smith, I. J., & Langhorne, P. J. (2016). The response of the Southern Ocean and Antarctic sea ice to freshwater from ice shelves in an earth system model. *Journal of Climate*, *29*(5), 1655–1672. https://doi.org/10.1175/JCLI-D-15-0501.1

Pauling, A. G., Smith, I. J., Langhorne, P. J., & Bitz, C. M. (2017). Time-dependent freshwater input from ice shelves: Impacts on Antarctic Sea ice and the Southern Ocean in an earth system model. *Geophysical Research Letters*, *44*(20), 10454–10461. https://doi.org/10.1002/2017GL075017

Polvani, L. M., & Smith, K. L. (2013). Can natural variability explain observed Antarctic sea ice trends? New modeling evidence from CMIP5. *Geophysical Research Letters*, *40*(12), 3195–3199. https://doi.org/10.1002/grl.50578

Purich, A., England, M. H., Cai, W., Chikamoto, Y., Timmermann, A., Fyfe, J. C., et al. (2016). Tropical pacific SST drivers of recent Antarctic sea ice trends. *Journal of Climate*, *29*(24), 8931–8948. https://doi.org/10.1175/JCLI-D-16-0440.1

Raphael, M. N., Holland, M. M., Landrum, L., & Hobbs, W. R. (2019). Links between the Amundsen Sea low and sea ice in the Ross Sea: Seasonal and interannual relationships. *Climate Dynamics*, *52*(3–4), 2333–2349. https://doi.org/10.1007/s00382-018-4258-4

Rignot, E., Jacobs, S., Mouginot, J., & Scheuchl, B. (2013). Ice-shelf melting around Antarctica. *Science*, *341*(6143), 266–270. https://doi.org/10.1126/science.1235798

Rignot, E., Mouginot, J., Scheuchl, B., van den Broeke, M., van Wessem, M. J., & Morlighem, M. (2019). Four decades of Antarctic ice sheet mass balance from. *Proceedings of the National Academy of Sciences of the United States of America*, *116*(4), 1095–1103. https://doi.org/10.1073/pnas.1812883116

Roquet, F., Ferreira, D., Caneill, R., Schlesinger, D., & Madec, G. (2022). Unique thermal expansion properties of water key to the formation of sea ice on Earth. *Science Advances*, *8*(46), eabq0793. https://doi.org/10.1126/sciadv.abq0793

Rye, C. D., Marshall, J., Kelley, M., Russell, G., Nazarenko, L. S., Kostov, Y., et al. (2020). Antarctic glacial melt as a driver of recent southern ocean climate trends. *Geophysical Research Letters*, *47*(11), 1–9. https://doi.org/10.1029/2019GL086892

Shu, Q., Wang, Q., Song, Z., Qiao, F., Zhao, J., Chu, M., & Li, X. (2020). Assessment of sea ice extent in CMIP6 with comparison to observations and CMIP5. *Geophysical Research Letters*, *47*(9), 1–9. https://doi.org/10.1029/2020GL087965

Si, Y., Stewart, A. L., & Eisenman, I. (2021). Coupled ocean/sea ice dynamics of the Antarctic slope current driven by topographic eddy suppression and sea ice momentum redistribution. *Journal of Physical Oceanography*, *52*(7), 1563–1589. https://doi.org/10.1175/JPO-D-21-0142.1

Stewart, A. L., Klocker, A., & Menemenlis, D. (2018). Circum-Antarctic shoreward heat transport derived from an eddy- and tide-resolving simulation. *Geophysical Research Letters*, *45*(2), 834–845. https://doi.org/10.1002/2017GL075677

Stewart, A. L., Klocker, A., & Menemenlis, D. (2019). Acceleration and overturning of the Antarctic slope current by winds, eddies, and tides. *Journal of Physical Oceanography*, *49*(8), 2043–2074. https://doi.org/10.1175/JPO-D-18-0221.1

Stewart, K. D., & Haine, T. W. N. (2016). Thermobaricity in the transition zones between alpha and beta oceans. *Journal of Physical Oceanography*, *46*(6), 1805–1821. https://doi.org/10.1175/JPO-D-16-0017.1

Swart, N. C., & Fyfe, J. C. (2013). The influence of recent Antarctic ice sheet retreat on simulated sea ice area trends. *Geophysical Research Letters*, *40*(16), 4328–4332. https://doi.org/10.1002/grl.50820

Thompson, A. F., Speer, K. G., & Chretien, L. M. S. (2020). Genesis of the Antarctic slope current in west Antarctica supplementary material. *Geophysical Research Letters*, *47*(16), e2020GL087802. https://doi.org/10.1029/2020GL087802

Turner, J., Comiso, J. C., Marshall, G. J., Lachlan-Cope, T. A., Bracegirdle, T., Maksym, T., et al. (2009). Non-annular atmospheric circulation change induced by stratospheric ozone depletion and its role in the recent increase of Antarctic sea ice extent. *Geophysical Research Letters*, *36*(8), 1–5. https://doi.org/10.1029/2009GL037524

Wingham, D. J., Shepherd, A., Muir, A., & Marshall, G. J. (2006). Mass balance of the Antarctic ice sheet. *Philosophical Transactions of the Royal Society A: Mathematical, Physical & Engineering Sciences*, *364*(1844), 1627–1635. https://doi.org/10.1098/rsta.2006.1792

Wunsch, C., Heimbach, P., Ponte, R. M., & Fukumori, I. (2009). Global general circulation of the ocean estimated by the ECCO-consortium. *Oceanography*, *22*(2), 88–103. https://doi.org/10.5670/oceanog.2009.41

Zunz, V., Goosse, H., & Massonnet, F. (2013). How does internal variability influence the ability of CMIP5 models to reproduce the recent trend in Southern Ocean sea ice extent? *The Cryosphere*, *7*(2), 451–468. https://doi.org/10.5194/tc-7-451-2013

Zweng, M. M., Reagan, J. R., Antonov, J. I., Mishonov, A. V., Boyer, T. P., Garcia, H. E., et al. (2013). *World Ocean Atlas 2013, vol. 2, salinity* (Vol. 2, p. 39). NOAA Atlas NESDIS.